Nonisothermal decomposition of CdC_2O_4–FeC_2O_4 mixtures in air

El-H.M. Diefallah[a,*], M.A. Gabal[a], A.A. El-Bellihi[b], N.A. Eissa[c]

[a]*Department of Chemistry, Faculty of Science, Zagazig University, Benha-Branch, Kalyobia, Egypt*
[b]*Department of Chemistry, Faculty of Science, King Abdulaziz University, Jeddah, Egypt*
[c]*Department of Chemistry, Faculty of Science, Al Azhar University, Cairo, Egypt*

Abstract

DTA–TG, XRD, and [57]Fe Mössbauer spectral measurements were used to study the thermal decomposition reactions of the system CdC_2O_4–FeC_2O_4 (1:2 mole ratio) in air. The results showed that the thermal oxidative decomposition of each metal oxalate in the mixture occurs in one TG step and that oxide spinel is formed at 800°C. Mössbauer spectra of samples showed that the iron(III) oxide formed in the early stages of the decomposition at 250°C is mainly fine-grained and as the temperature is increased, well-crystalline hematite is formed. Above 250°C, the Mössbauer spectrum showed the typical six-line pattern of magnetically oriented Fe(III) oxide, but at 800°C, the spectrum showed quadrupole interaction characteristic of $CdFe_2O_4$ spinel. Kinetic analysis of the nonisothermal data according to the integral composite method showed that the oxidation and decomposition of FeC_2O_4 to Fe_2O_3 and CO_2 and of CdC_2O_4 to CdO and CO_2 are best described by the three-dimensional phase boundary (R_3) model. The activation parameters for both decomposition steps were calculated and discussed.
© 2001 Elsevier Science B.V. All rights reserved.

Keywords: Decomposition; Thermal analysis; Mössbauer; Cadmium oxalate; Iron(II) oxalate

1. Introduction

In the past three decades, increased attention has been paid to the chemistry and physics of mixed oxide systems containing iron ions [1–3]. These oxides are characterized by specific electric, magnetic, piezo-electric or some other physical properties. Their specific physical behavior, in relation to other materials, is a consequence of their chemical behavior and structure. Significant attention has been paid to the investigation of the chemical and structural properties of hematite, α-Fe_2O_3 [1,2], in which some iron ions are substituted by other metal ions. These systems have been investigated using different experimental techniques, such as XRD, FT-IR, and Mössbauer spectroscopy.

Studies of the thermal analysis and kinetics of the thermal decomposition of metal oxalates have drawn the interest of several investigators [4–8], since the thermal decomposition of such materials results in products, e.g. oxides or metals, which may possess pores, lattice imperfections, and other characteristics necessary for its function as reactive solids [9]. The behavior of the thermal decomposition and stability of salts of simple metal oxalates have been reviewed [6]. Dollimore et al. [4,5] studied the thermal decomposition of $CdC_2O_4 \cdot 3H_2O$ and the results showed that the end product in nitrogen is Cd metal and in air is CdO. Thermal decomposition of $FeC_2O_4 \cdot 2H_2O$ was investigated in air, oxygen, and inert atmospheres, using DTA–TG, Mössbauer spectroscopy, and XRD technique [10].

* Corresponding author. Fax: +20-13-222-578.
E-mail address: mabrouk@yalla.com (El.-H.M. Diefallah).

XRD analysis showed that the final decomposition product in air is Fe_2O_3 and in N_2 the residue heated at 630°C was found to be free iron, Fe_3O_4, and trace of FeO [11].

The thermal behavior in air and nitrogen of the mixed metal oxalates [7,8], $MCu(C_2O_4)_2 \cdot xH_2O$, where M = Fe, Ni, or Co has been examined using TG, TM, DSC, and EGA techniques, where it is found that the thermal behavior of mixed metal oxalates differed from that of the individual metal oxalates. Schuele [12] prepared ferromagnetic and ferrimagnetic fine particles of mixed oxides by suitable heat treatment of coprecipitated oxalates of Co–Fe, Ni–Fe, and Cu–Fe systems in a wide range of compositions. Basahel et al. studied DTA–TG behavior of coprecipitated iron(III) oxalate–magnesium oxalate mixture and found that magnesium ferrite is formed in samples heated at higher temperatures.

The Mössbauer spectroscopy has been successfully applied in combination with thermal analysis to investigate the changes in the valence states of iron during the thermal decomposition of some iron oxalate compounds. Gallagher and Khurkjian [13] used the Mössbauer effect to follow the thermal decomposition of ferric oxalate and alkaline earth trioxalatoferrate(III) and minor changes in the oxidation state of iron. Diefallah et al. [14] studied the Mössbauer spectra of samples of ammonium trioxalatoferrate(III) trihydrate calcined at different temperatures and the results showed that in the early stages of the decomposition part of the Fe(III) oxide is formed in a superaparamagnetic doublet state.

In the present study, the thermal decomposition of cadmium oxalate–ferrous oxalate (1:2 mole ratio) in air has been studied using DTA–TG, XRD, and [57]Fe Mössbauer effect measurement. Kinetic analysis of nonisothermal results of the decomposition reactions in the mixture were carried out using various solid-state reaction model equations and integral methods of dynamic data analysis.

2. Experimental

Pure oxalates, $CdC_2O_4 \cdot 3H_2O$ and $FeC_2O_4 \cdot 2H_2O$, were prepared by precipitation with AR oxalic acid from aqueous solutions of the AR salt sulfates. The fine particles were filtered, washed with distilled water

until free of sulfate ion and dried. The oxalate mixture, $CdC_2O_4 \cdot 3H_2O$–$FeC_2O_4 \cdot 2H_2O$ (1:2 mole ratio) was prepared by the impregnation technique by thoroughly mixing the desired mole ratio of pure oxalates, then the mixture was dried in a thermostated oven at 50°C for 2 h.

Simultaneous DTA–TG experiments were performed using Shimadzu DT-40 thermal analyzer. Experiments were carried out in air at flow rate of $3.0 \, l \, h^{-1}$ against α-alumina as a reference at heating rates of 1, 2, 3, and 5°C min^{-1}. The sample mass in the Pt cell of the thermal analyzer was kept at about 8 mg in all experiments in order to ensure a linear heating rate and accurate temperature measurements. Samples of cadmium oxalate–ferrous oxalate mixture were thermally heated in an electric oven for 30 min at 250°C, for 1 h at 400°C or for 2 h at 800°C. The samples were then removed from the oven and cooled in air in a desiccator to room temperature. X-ray diffraction patterns for the samples calcined at different temperatures were recorded using a Philips 1710 X-ray diffraction unit using a Co target and Ni filter. Mössbauer spectra of the samples calcined at different temperatures were determined at room temperature relative to metallic iron as a reference using a MS 900 Ranger Scientific Co. with [57]Co–Rh source.

3. Results and discussion

Fig. 1 shows the DTA–TG curves obtained for the physical mixture, $CdC_2O_4 \cdot 3H_2O$–$FeC_2O_4 \cdot 2H_2O$ (1:2 mole ratio) in air. The DTA–TG curves showed that the complete decomposition of the hydrated mixture occurs in four steps at temperature below 400°C. The first step starts at about 62°C and is characterized by a broad endothermic peak at 90°C accompanied by a weight loss of 9% in agreement with calculated weight loss of 8.8% which is attributed to the loss of water of crystallization of cadmium oxalate in the mixture. This dehydration step was found to be complete at about 100°C and the mixture was stable up to 140°C. The second step shows also a broad endothermic peak at about 172°C accompanied by a weight loss of 12.5% due to the dehydration of ferrous oxalate in the mixture (calculated weight loss 11.7%). This step is complete at about 182°C. The third step follows immediately after the second step and shows a weight
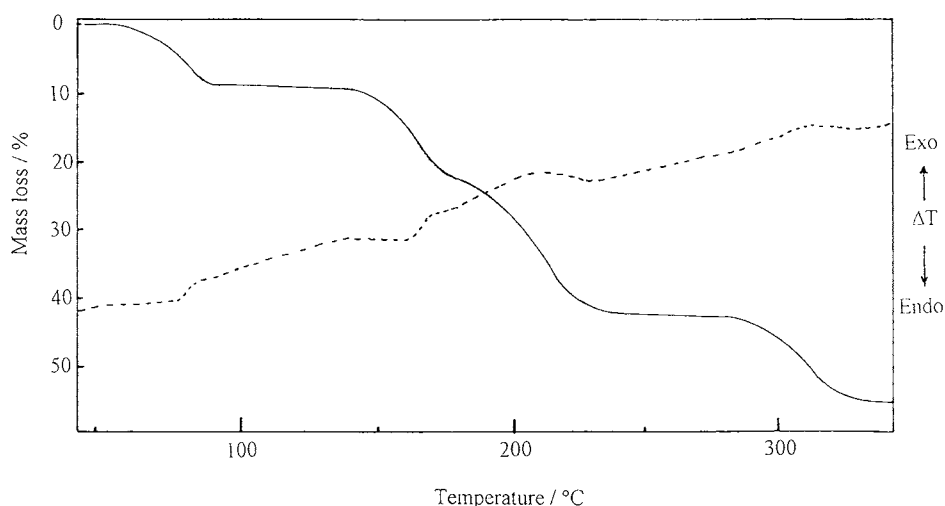
Fig. 1. DTA–TG curves of $CdC_2O_4 \cdot 3H_2O$–$FeC_2O_4 \cdot 2H_2O$ (1:2 mole ratio) mixture in air.

loss of 21.5% at about 250°C compared with the calculated weight loss of 22.5% due to the oxidation and decomposition of the anhydrous ferrous oxalate in the mixture and formation of CdC_2O_4–Fe_2O_3. A very broad exothermic peak at about 220°C characterizes this step. The mixture is thermally stable up to about 290°C, where the fourth step begins. This step shows a weight loss of 11% in accordance with the calculated weight loss of 10% due to the decomposition of CdC_2O_4 and the formation of the oxide mixture, CdO–Fe_2O_3. This step was characterized by broad exothermic peak at about 325°C due to air oxidation of CO to CO_2 (6). In general, the DTA–TG behavior of cadmium and ferrous oxalates in the mixture is similar to that of the pure salts [5,15], so that the thermal decomposition behavior of the salts is not much affected by their presence in the mixture.

The results obtained using XRD measurements are in agreement with the results from DTA–TG experiments. The starting material gave XRD pattern which generally agrees with the results reported in the ASTM data cards for the hydrated oxalates of Cd and Fe(II) oxalates. The sample calcined at 250°C shows XRD pattern characteristic of anhydrous cadmium oxalate and at the same time none of the XRD lines are characteristic of Fe_2O_3 crystallites. This indicates that the oxide formed at this temperature is microcrystalline (or possibly even amorphous). For samples calcined at 400°C, the XRD lines are characteristic for

the presence of oxide mixture of both CdO and well-crystalline Fe_2O_3, and no intensive XRD lines due to the spinel oxide were observed. For the sample calcined at 800°C for 2 h, XRD lines show the presence of CdO, Fe_2O_3, and $CdFe_2O_4$ spinel. Upon rising the calcination time to several hours at 800°C, only XRD lines characteristic of $CdFe_2O_4$ spinel appear.

Mössbauer spectra recorded at room temperature of samples calcined at different temperatures are shown in Fig. 2. The spectrum of the noncalcined sample (curve (a)) shows an isomer shift of 1.23 mm s^{-1} and quadrupole splitting of 1.62 mm s^{-1} characteristic of $FeC_2O_4 \cdot 2H_2O$ [16]. For samples calcined at 250°C, the Mössbauer spectrum (curve (b)) showed a doublet owing to quadrupole interaction due to the formation of very fine particles of paramagnetic Fe_2O_3 having colloidal dimensions. The results obtained are in agreement with the results of the XRD patterns and those reported by Nakamura et al. [17] for Fe(III) oxide prepared by the thermal decomposition of α-Fe(III) oxide hydrate. The spectrum for samples calcined at 400°C (curve (c)) shows that the calcination product consists of two Fe(III) oxides, one is formed with 25.8% and having a supermagnetic doublet ($\Delta E_Q = 0.735$ mm s^{-1}) and an isomer shift ($\delta = 0.368$ mm s^{-1}), and the other exhibits a magnetic hyperfine splitting of 509 kOe which is significantly less than the value of Fe(III) oxide of 515 kOe [13]. The spectrum for samples calcined at 800°C
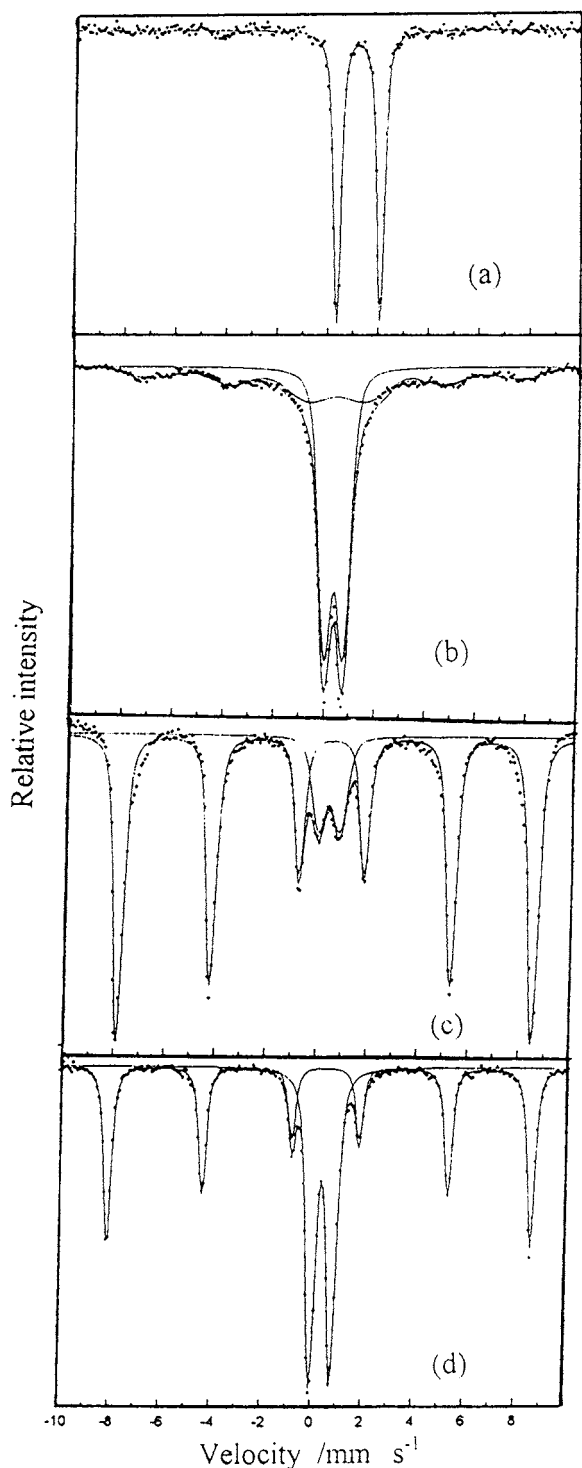
Fig. 2. Mössbauer spectra of $CdC_2O_4 \cdot 3H_2O$–$FeC_2O_4 \cdot 2H_2O$ (1:2 mole ratio) mixture calcined at different temperatures: (a) ambient temperature; (b) 250°C; (c) 400°C; (d) 800°C.

(curve (d)) shows a doublet having an isomer shift ($\delta = 0.357$ mm s^{-1}) and a quadrupole splitting ($\Delta E_Q = 0.735$ mm s^{-1}) characteristic of $CdFe_2O_4$ [18], in addition to a hextet having a magnetic hyperfine splitting due to α-Fe_2O_3 and having a magnetic splitting of 517 kOe consistent with the normal value for Fe(III) oxide with the larger particle size. Upon increasing the calcination time at 800°C, the percentage of ferrite spinel increases. These results are in agreement with the results of the XRD data.

The kinetics of the oxalate decomposition steps (viz. the third and fourth decomposition steps) were studied under dynamic conditions at heating rates 1, 2, 3, and 5°C min^{-1}. Kinetic analysis of the dynamic TG curves were carried out using three integral methods: Ozawa [19], Coats–Redfern [20], and Diefallah composite method [21]. Fig. 3 shows the fractional reaction remaining as a function of temperature for the decomposition in air of FeC_2O_4 to Fe_2O_3 (Fig. 3a) and of CdC_2O_4 to CdO (Fig. 3b) in their mixture at different heating rates. The composite method of analysis was used to perform a complete analysis of all nonisothermal curves into a single master curve [3,14,21–29]. The method employs multiple sets of nonisothermal data and uses all (α, T, β_i) values obtained at the different heating rates, β_i. The use of single-heating rate methods should be very limited and the application of multiset methods is expected to enrich kinetics with a deeper insight into the multistep nature of solid-state reactions [30–32]. In many cases, the activation energies estimated by the composite method are, within experimental errors, in good agreement with the values estimated using the model-free method of Ozawa [3,14,21–26]. Vyazovkin and Wight [33] pointed out that the use of the model-free approach is a trustworthy way of obtaining reliable results from both nonisothermal and isothermal data. Although, the composite method of integral analysis of nonisothermal data involves a model-fitting kinetic approach, however it does not assume a particular reaction model, but it allows us to choose the model function that gives the best representation of all (α, T, β_i) values obtained at the different heating rate experiments. Deviations from a straight line relationship are interpreted in terms of multistep reaction mechanism [19,21,34].

The integral form of the equation showing the dependence of the kinetic model function $g(\alpha)$ on
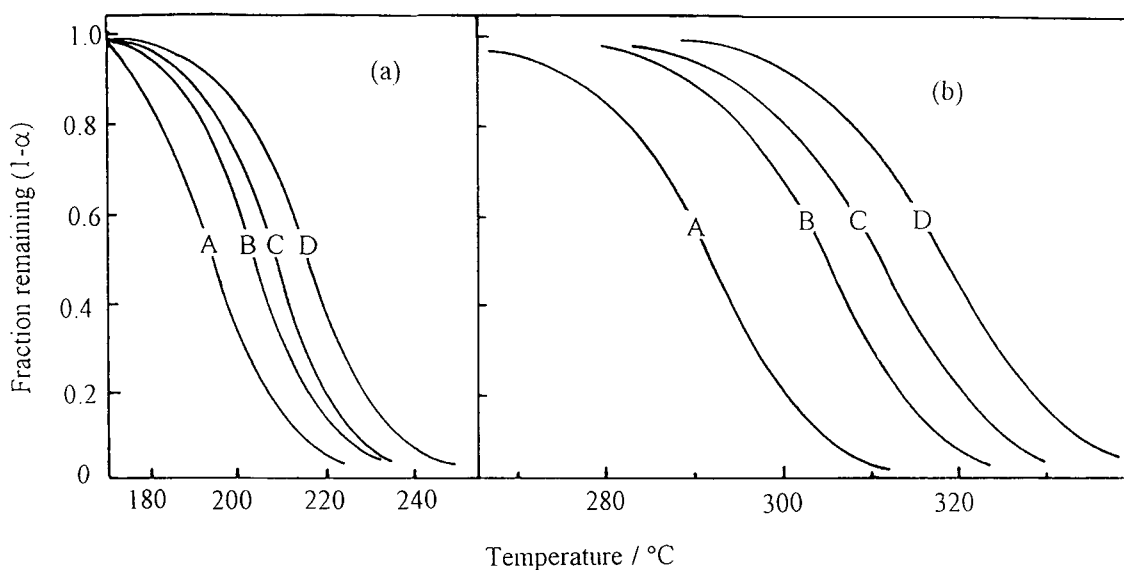
Fig. 3. Dynamic measurements for the thermal decomposition of $CdC_2O_4 \cdot 3H_2O$–$FeC_2O_4 \cdot 2H_2O$ (1:2 mole ratio) mixture in air: (a) decomposition of FeC_2O_4 to Fe_2O_3; (b) decomposition of CdC_2O_4 to CdO. Heating rate: curve (A), 1°C min^{-1}; curve (B), 2°C min^{-1}; curve (C), 3°C min^{-1}; curve (D), 5°C min^{-1}.

temperature is rewritten in the form which allows making a plot of all nonisothermal data into a master curve for the correct reaction model. For example, Doyle's equation [35] is rewritten in the form:

$$\log g(\alpha)\beta = \left[\log\left(\frac{AE}{R}\right) - 2.315\right] - 0.4567\frac{E}{RT}$$

where $g(\alpha)$ is the kinetic model function, β the heating rate (°C min^{-1}), α the fractional reaction, A the frequency factor, and E the activation energy of the reaction. The dependence of $\log g(\alpha)\beta$, calculated for the different α values at their respective β values, on $1/T$ must give rise to a single master straight line for the correct form of $g(\alpha)$. In a similar way, the modified Coats–Redfern equation [20] is rewritten in the form:

$$\ln\left[\frac{\beta g(\alpha)}{T^2}\right] = \ln\left(\frac{AR}{E}\right) - \frac{E}{RT}$$

Hence, the dependence of $\ln[\beta g(\alpha)/T^2]$ calculated for different α values at their respective β values on $1/T$ must give rise to a single master straight line for the correct form of $g(\alpha)$, and a single activation energy and frequency factor can be readily calculated. Similarly, when using approximate equation of Madhusudanan

et al. [36], the equation for composite analysis has the form:

$$-\ln\left[\frac{g(\alpha)}{T^{1.921503}}\right] = -\ln\left(\frac{AR}{E}\right) + 3.7720501$$
$$- 1.921503\ln E - \frac{E}{RT}$$

Hence, the dependence of the left side of this equation on $1/T$ should give rise to a master straight line for the correct form of $g(\alpha)$ for all nonisothermal data.

Kinetic analysis of data according to the composite method using the multiple sets of nonisothermal data obtained at different heating rates showed that the two oxalate decomposition steps are best described by phase boundary (R_2 and R_3), first order (F_1), and random nucleation (A_2) models. Fig. 4 shows the composite analysis of dynamic TG data based on Doyle's equation in accordance with the R_3 model function. Fig. 5 shows a plot of the activation energies estimated by the Ozawa method versus α with 0.05 α step. There is irregular variations in E with α. The average activation parameters according to the three computational methods for the two decomposition steps are summarized in Table 1. The three methods of calculation show, within experimental error, similar

A

B
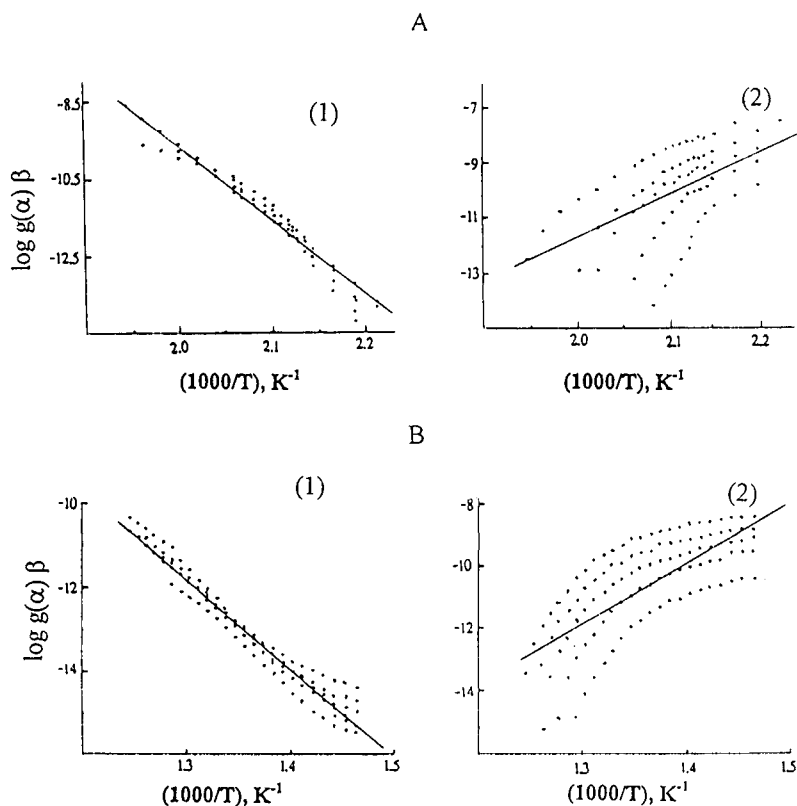
Fig. 4. Composite analysis of TG data for the nonisothermal decomposition in air of (A) FeC$_2$O$_4$, and (B) CdC$_2$O$_4$ in their mixture based on Doyle's equation assuming (1) R$_3$ model, and (2) E$_1$ model.

activation parameters for the thermal decomposition of FeC$_2$O$_4$. The values calculated by the Ozawa method for the step of decomposition of CdC$_2$O$_4$ are less than that calculated by the other two methods. However, the results generally show that the average activation energy for the oxidative decomposition of FeC$_2$O$_4$ is higher than that for the oxidative decomposition of CdC$_2$O$_4$. Fig. 5 shows approximately constant E with α and the composite method of analysis showed a single master straight line for all

(α, T, β_i) values obtained at different heating rate experiments for each of FeC$_2$O$_4$ and CdC$_2$O$_4$ thermal decomposition, so that it is likely that the rate-limiting step in both cases is a single reaction step.

Mohamed and Galwey [37] found that the activation energy for the thermal decomposition of FeC$_2$O$_4$ equals 175 ± 7 kJ mol^{-1} and that it is comparable with the values for the decomposition of other divalent oxalates, so that the energy barrier to anion breakdown is the strength of the bond between the ferrous iron and

Table 1
Activation parameters of the nonthermal decomposition in air of FeC$_2$O$_4$ and CdC$_2$O$_4$ in their mixture calculated according to the R$_2$ model

Method of analysis	Decomposition of FeC$_2$O$_4$		Decomposition of CdC$_2$O$_4$	
	E (kJ mol^{-1})	log A (min^{-1})	E (kJ mol^{-1})	log A (min^{-1})
Composite method	132 ± 2	12.9 ± 0.4	217 ± 6	18.1 ± 1.0
Coats–Redfern	130 ± 7	12.1 ± 0.8	187 ± 19	19.6 ± 1.5
Ozawa	137 ± 8	13.4 ± 0.9	159 ± 3	12.8 ± 0.3
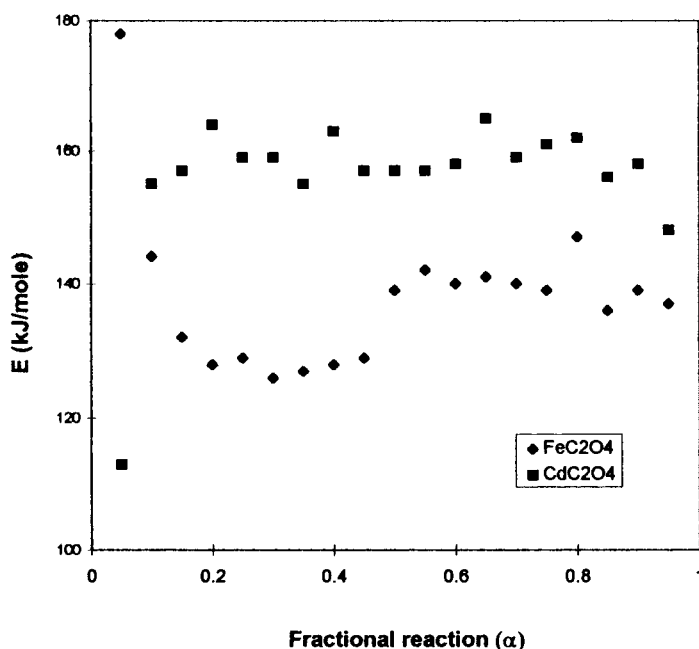
Fig. 5. Plots of the activation energies vs. α calculated by the Ozawa method for the oxidative decomposition of FeC_2O_4 and CdC_2O_4 in CdC_2O_4–FeC_2O_4 (1:2 mole ratio).

the carboxyl oxygen. In air, the process of cation oxidation (Fe^{2+} to Fe^{3+}) follows the breakdown of the oxalate anion and leads to the formation of Fe_2O_3 as the final product [10]. The electronegativity of Fe (1.83) is more than that of Cd (1.69) [38] so that the addition of cadmium ions to FeC_2O_4 results in an increased positive on the iron ion, and a less covalent type of bond thus occurs in the mixed oxalate than in pure FeC_2O_4 [8]. This results in a weakening of the Fe–O bond and a lowering in the activation energy of FeC_2O_4 decomposition.

In CdC_2O_4–FeC_2O_4, the activation energy for the thermal decomposition of cadmium oxalate is much higher than that of the Fe(II) oxalate. The radius of Cd(II) (97 pm) is larger than that of Fe(II) (76 pm), so that Fe(II) would have a stronger metal–oxygen bond than Cd(II). The decomposition of Cd(II) oxalate in nitrogen gives Cd metal and the decomposition of Fe(II) oxalate gives Fe, Fe_3O_4, and trace of FeO. In air, the metal powder formed in the decomposition is oxidized to metal oxide. As the M–O_I bond strength increases, the C–O_I bond (in $M \begin{smallmatrix} O_I - C = O_{II} \\ O_I - C = O_{II} \end{smallmatrix}$) becomes weaker [39]. This would allow ease of rupture of C–O_I

bond in Fe(II) oxalate than in Cd(II) oxalate and would cause an increase in activation energy in the latter than the former. When rupture of C–O_I bond occurs in Fe(II) oxalate, it will be followed by rupture of the second M–O_I bond, leading to the metal oxide. At the higher temperature, rupture of the two M–O_I bonds in Cd(II) oxalate produces the metal followed in air by its oxidation to the oxide. In addition, the exothermicity of the iron oxalate decomposition step is higher than that of cadmium oxalate and this would lower the activation energy for the decomposition of the former than that of the latter.

References

[1] S. Music, S. Popvic, S. Dalipi, J. Mater. Sci. 28 (1993) 1793.
[2] M. Ristic, S. Popovic, M. Ristic, J. Mater. Sci. 28 (1993) 632.
[3] S.N. Basahel, A.A. El-Bellihi, M. Gabal, El-H.M. Diefallah, Thermochim. Acta 256 (1995) 339.
[4] D. Dollimore, D.L. Griffiths, D. Nicholson, J. Chem. Soc. (1963) 2617.
[5] D. Dollimore, D.L. Griffiths, J. Therm. Anal. 2 (1970) 229.
[6] D. Dollimore, Thermochim. Acta 117 (1987) 331.

[7] A. Coetzee, D.J. Eve, M.E. Brown, J. Therm. Anal. 39 (1993) 947.

[8] A. Coetzee, M.E. Brown, D.J. Eve, C.A. Strydom, J. Therm. Anal. 41 (1994) 357.

[9] V.V. Boldyrev, M. Bulens, B. Delmon, The Control of the Reactivity of Solids, Elsevier, Amsterdam, 1979.

[10] B. Boyanov, D. Khadzhiev, V. Vasilev-Plavdiv, Thermochim. Acta 93 (1985) 89.

[11] D. Broadbent, D. Dollimore, J. Dollimore, J. Chem. Soc. (1967) 451.

[12] W.J. Schuele, J. Chem. Phys. 63 (1959) 83.

[13] P.K. Gallagher, C.R. Khurkjian, Inorg. Chem. 5 (1966) 214.

[14] El-H.M. Diefallah, S.N. Basahel, A.A. El-Bellihi, Thermochim. Acta 290 (1996) 123.

[15] E.D. Macklen, J. Inorg. Nuclear Chem. 29 (1967) 1229.

[16] P.R. Brady, J.F. Duncan, J. Chem. Soc. (1964) 653.

[17] T. Nakamura, T. Shinjo, Y. Endoh, N. Yamamato, M. Shiga, Y. Nakamura, Phys. Lett. 12 (1964) 178.

[18] S. Garcia, E. Aishuler, Solid State Phys. 89 (1985) 427.

[19] T. Ozawa, J. Therm. Anal. 2 (1970) 301.

[20] A.W. Coats, J.P. Redfern, Nature 20 (1964) 68.

[21] El-H.M. Diefallah, Thermochim. Acta 202 (1992) 1.

[22] El-H.M. Diefallah, A.A. El-Bellihi, S.N. Basahel, M. Abdel Wahab, Z.A. Omran, Thermochim. Acta 230 (1993) 143.

[23] El-H.M. Diefallah, A.Y. Obaid, A.H. Qusti, A.A. El-Bellihi, M. Abdel Wahab, M.M. Moustafa, Thermochim. Acta 274 (1996) 165.

[24] S.A. Al-Thabaiti, A.A. El-Bellihi, M.M. Moustafa, A.Y. Obaid, A.O. Alyoubi, A.A. Samarkandy, El-H.M. Diefallah, JKAU: Sci. 10 (1998) 103.

[25] A.Y. Obaid, A.O. Alyoubi, A.A. Samarkandy, S.A. Al-Thabaiti, S.A. Al-Juaid, A.A. El-Bellihi, El-H.M. Diefallah, J. Therm. Anal. Cal. 61 (2000) 989.

[26] El-H.M. Diefallah, M.A. Mousa, A.A. El-Bellihi, El-S. El-Mossalamy, G.A. El-Sayed, M.A. Gabal, J. Anal. Appl. Pyrl., 2001, in press.

[27] S.N. Basahel, A.A. El-Bellihi, El-H.M. Diefallah, J. Therm. Anal. 39 (1993) 87.

[28] A.A. El-Bellihi, J. Therm. Anal. 41 (1994) 191.

[29] S.N. Basahel, M.M. El-Fass, A.A. El-Bellihi, E.A. Al-Sabban, El-H.M. Diefallah, Radiat. Phys. Chem. 44 (1994) 583.

[30] M. Maciejewski, Thermochim. Acta 355 (2000) 145.

[31] S. Vyazovkin, Thermochim. Acta 355 (2000) 155.

[32] A.K. Burnham, Thermochim. Acta 355 (2000) 165.

[33] S. Vyazovkin, C.A. Wight, Thermochim. Acta 340/341 (1999) 53.

[34] M.E. Brown, M. Maciejewskj, S. Vyazovkin, R. Nomen, J. Sempere, A. Burnham, J. Opfermann, R. Strey, H.L. Anderson, A. Kemmler, R. Kenleers, J. Janssens, H.O. Desseyn, C.-R. Li, T.B. Tang, B. Roduit, J. Malek, T. Mitsuhashi, Thermochim. Acta 255 (2000) 125.

[35] D. Doyle, J. Appl. Polym. Sci. 5 (1961) 285.

[36] P.M. Madhusudanan, K. Krishnan, K.N. Ninan, Thermochim. Acta 97 (1986) 189.

[37] M.A. Mohamed, A.K. Galwey, Thermochim. Acta 213 (1993) 269.

[38] A.L. Allred, J. Inorg. Nuclear Chem. 17 (1961) 215.

[39] J. Fojita, J. Phys. Chem. 61 (1957) 1014.